

# Acoustic Holographic Imaging by Scanning Point Contact Excitation and Detection in Piezoelectric Materials

Evgeny TWERDOWSKI, Moritz VON BUTTLAR, Anowarul HABIB, Reinhold WANNEMACHER, Wolfgang GRILL, Experimental Physics II, University of Leipzig, Germany

**Abstract.** Excitation and detection of ultrasound in piezoelectric single crystals by scanning electrical point contacts is employed for the imaging of volume acoustic wave propagation. Results are demonstrated for a Z-cut lithium niobate single crystal. The Coulomb excitation scheme leads to a predictable point excitation and detection. Short pulse excitation together with full transient signal recording allows for spatially and temporally resolved holographic imaging. The holography data can serve as an input for modeling of the effective elastic tensor and the piezoelectric properties of the materials under investigation.

## 1. Introduction

The direction of energy propagation for an elastic wave in an elastically anisotropic material is in general not collinear with its wave vector. A vibration wavefront emanating from a point source on the surface of such a material is not spherical. Moreover, there exist directions, also known as caustics or phonon focusing, in which the energy flow becomes very large (infinite in the limit of geometric acoustics).

The study of the phonon focusing phenomenon in single crystals has attracted great attention in the last few decades [1-8]. Ultrasonic holographic imaging is one of the techniques utilized that can operate at ambient temperatures and is also applicable to metals and noncrystalline anisotropic materials. In one scheme, two ultrasonic transducers are focused on the opposite surfaces of the sample under investigation. To provide ultrasound coupling, the sample and the transducers are typically placed in a coupling fluid [9]. Alternatively, a focused laser serves to excite ultrasonic waves in the sample which are then detected interferometrically via reflection of another focused laser beam from the other side of the sample. The foci of the transducers, or of the laser beams, respectively, are treated in this case as ultrasound point sources and detectors [8].

For piezoelectric materials, one can employ a simple conducting point-like probe brought in contact with the material surface in order to detect a signal. A similar idea was utilized more than three decades ago for the probing of surface acoustic waves (SAW) in  $\text{LiNbO}_3$  [10]. In contrast to that, this paper deals with holographic imaging of bulk acoustic waves (both amplitude and phase information are acquired).

This paper demonstrates, using a  $\text{LiNbO}_3$  single crystal, that electric surface point excitation and similar detection can be employed for holographic imaging of the transport properties of acoustic waves in piezoelectric materials. The method has been applied, but is not limited, to single crystals. Time-evolving ultrasound wavefronts are recorded while

scanning the surface of the crystal. Simple geometrical acoustic considerations allow for identification of longitudinal, transverse and mode-converted waves.

## 2. Methods and Materials

The set-up of the experiment is presented in the left image of Fig. 1. A gold sphere of 300  $\mu\text{m}$  diameter was used as an excitation electrode. It was mounted at the contact point of two crossing glass fibers. The latter also acted as a spring which guaranteed contact between the electrode and the sample. The receiving electrode (a spring-loaded thin copper wire of 100  $\mu\text{m}$  thickness) was mounted in the copper plate using a plastic spacer. A motor-driven translation stage was employed to position the excitation electrode in two dimensions on the sample surface. It has to be noticed that a proper mechanical contact between the crystal and the grounded copper plate influenced considerably the signal amplitude detected. A small gap due to particle contamination or roughness of the surface resulted in a drastic drop of the detected signal amplitude, which was recognized by pressing the crystal and the plate together. The problem was rectified by putting a drop of distilled water between the crystal and the grounded plate resulting in an improvement of the detected signal amplitude by a factor of 30.

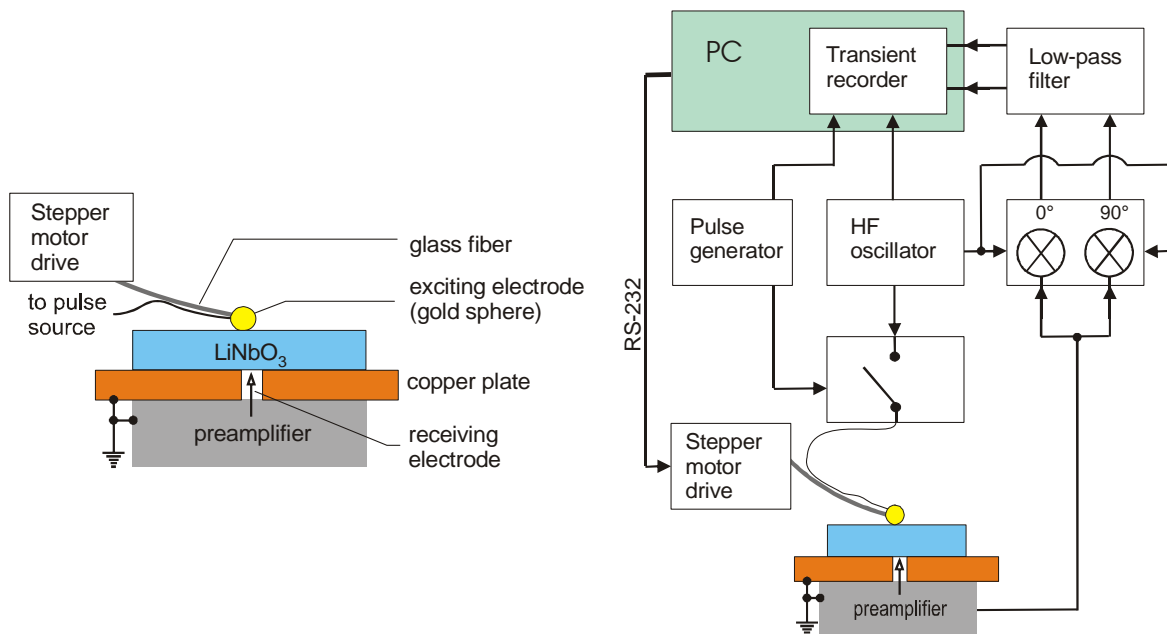


**Fig. 1** Experimental setup: sample mount (left) and electronic scheme (right).

The electrical scheme of the setup is presented in the right image of Fig. 1. High-frequency bursts were cut from a continuous wave train generated by a stabilized CW oscillator operated at 100 MHz. The received signal was preamplified by an operational amplifier with a FET-input and a bias current in the pA range to provide a high-impedance input. The wire connecting the receiving electrode and the input of the electronics was kept very short (5 mm) to keep input capacitance small. The preamplifier was placed in a HF-shielded case and powered from batteries.

In the receiving part of the electronics a quadrature detection method was employed. The preamplified signal was submitted to a two-channel multiplier. In the first channel the signal was multiplied by the reference CW signal used for the excitation burst. A time delay corresponding to a 90° phase shift was introduced to the reference CW signal by an additional cable, after which the signal was fed to the second multiplier. After filtering out

the high frequency components of the product signal, the low frequency components were acquired by a two-channel 100 MHz sampling rate transient recorder. From the two acquired waveforms, both amplitude and phase were determined using the Pythagorean theorem and the inverse tangent.

Application of the transient recorder offers an advantage over the signal acquisition scheme based on the time-selective boxcar technique [11]. The transient recorder allows for variable gating of the recorded signal in the post-processing stage, thus obtaining numerous images out of a single measurement that correspond to conventional gated C-scan information. Application of the time-selective detection based on boxcar technique would require a separate measurement for each position of the time gate. It should be noted, however, that due to analog integration the boxcar technique can provide better signal to noise characteristics than that based on transient recorder acquisition.

### 3. Results and discussion

Below selected results of holographic imaging for a Z-cut  $\text{LiNbO}_3$  crystal with a diameter of 25.4 mm and a thickness of 5.02 mm are presented. The width of the excitation burst was set to 53 ns. An example of the amplitude waveform acquired at one particular point on the sample surface is given in Fig. 2. Normally 250000 such transients are acquired during a single scan consisting of 500x500 pixels. The peaks correspond to the arrival of ultrasound waves of various modes and their multiple echoes. The observed patterns can be attributed to longitudinal and transverse acoustic waves by using literature values for the sound velocities.

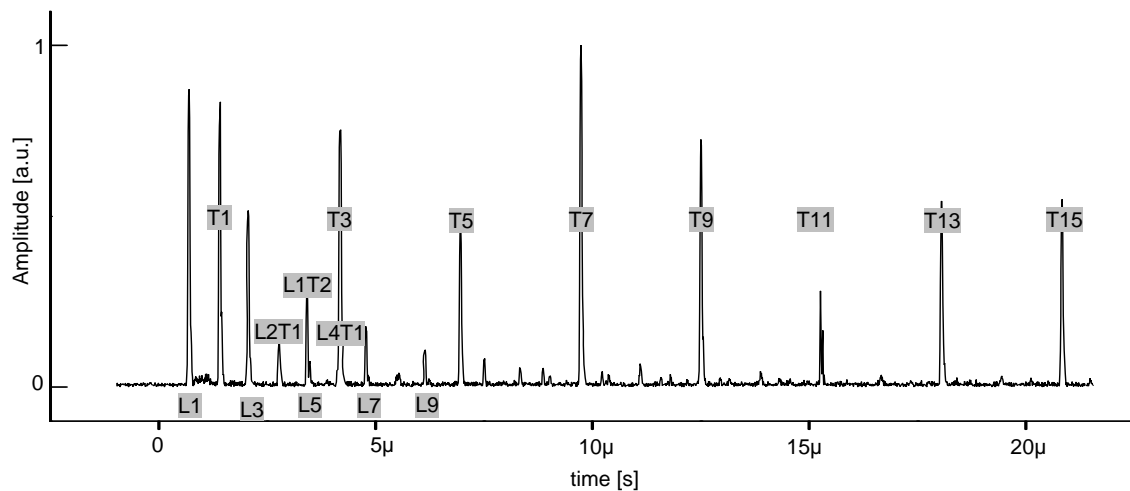


**Fig. 2** Amplitude waveform acquired at the center of the scan area. Duration of the excitation burst was 53 ns. Labels denote transverse (T), longitudinal (L), or mode-converted waves (LT). The number correspond states how often the crystal was traversed by particular mode. Some of the modes interfere due to arrival at nearly the same time (L5 and L1T2, T3 and L4T1).

### *Two-dimensional presentation of the acquired data*

After acquisition of the transients for each position of the scanner, time gating was performed in order to construct the snapshots of the ultrasound wave as it appears on the surface of the crystal. The earliest signal detected is the longitudinal wave (L1 in Fig. 2). This wave is not noticeably influenced by the anisotropy of the  $\text{LiNbO}_3$  crystal along the z-axis. The wavefront of this wave is therefore that of a spherical expanding wave, which is illustrated by the isolines of constant phase in the right image of Fig. 3.

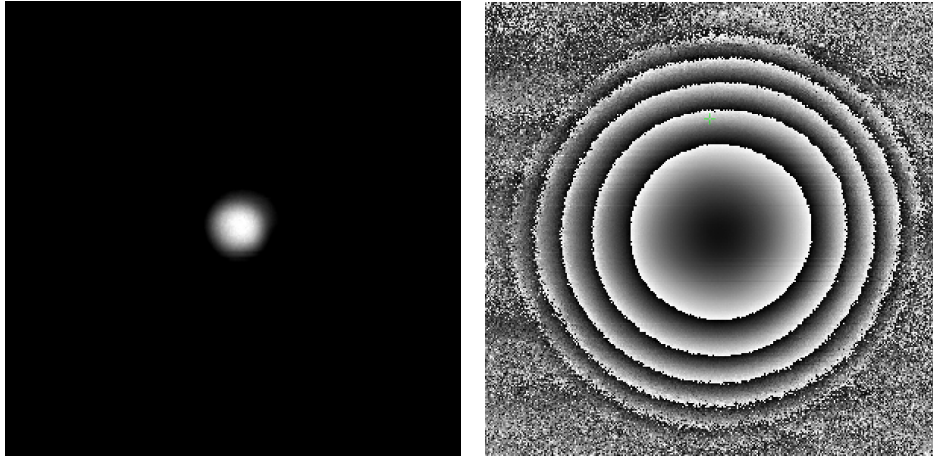


**Fig. 3** Hologram of the first transit signal for longitudinal polarization (L1 mode in Fig. 2) in  $\text{LiNbO}_3$ . Width of the images: 10 mm; left: representation of the magnitude with brightness proportional to the magnitude; right: representation of the phase with full gray scale proportional to  $2\pi$ .

The first transverse echo (T1 in Fig. 2) reflects the trigonal symmetry of the crystal (Fig. 4). This symmetry is destroyed in later echoes (left image in Fig. 5), which may be explained by a minor misalignment of the crystal axes relative to the sample surfaces or non-parallel surfaces and interference of the transverse waves with mode-converted waves. Mode conversion occurs at each reflection from one of the surfaces of the crystal. Such a converted mode is shown in the right image of Fig. 5 and corresponds to the L2T1-labelled spike in Fig. 2. Mode identification employed here is based on the time of flight of the acoustic modes in the crystal under consideration of its cut.

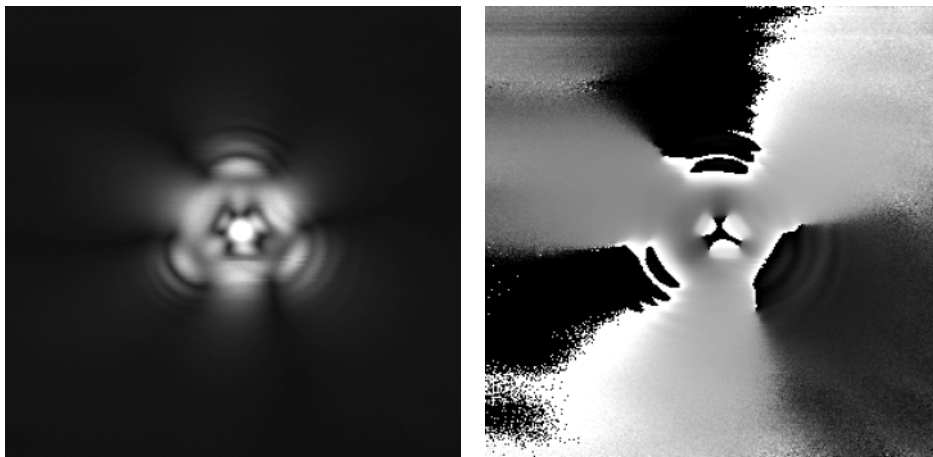


**Fig. 4** Hologram of the first transit signal for transverse polarization (T1 mode in Fig. 2) in  $\text{LiNbO}_3$ . Width of the images: 10 mm; left: representation of the magnitude with brightness proportional to the magnitude; right: representation of the phase with full gray scale proportional to  $2\pi$ .

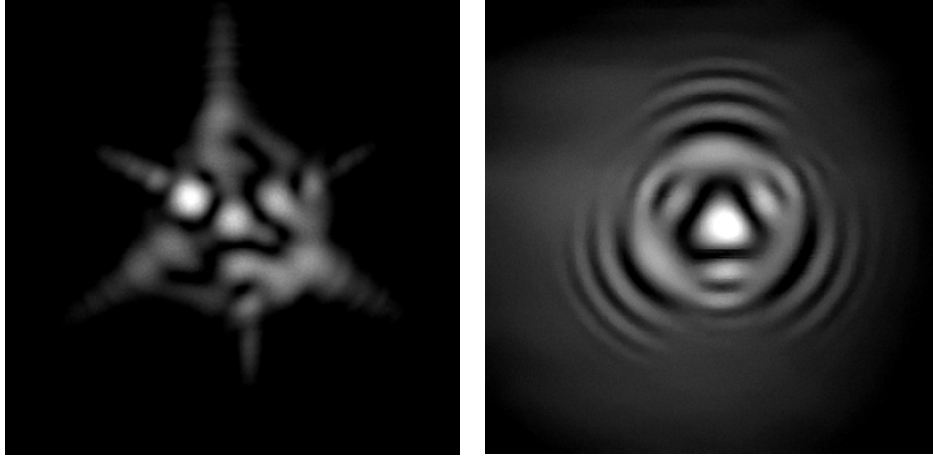


**Fig. 5** Left: magnitude of one of the later transversally polarized echoes (T7 in Fig. 2). Right: magnitude of mode converted waves (L2T1 mode in Fig. 2). The width of the image is 10 mm.

#### *Pseudo-3D presentation of the acquired data*

The images presented above correspond to two-dimensional time-snapshots of the ultrasonic wave as it appears on the surface of the crystal. The acquired data is three-dimensional (two dimensions for the position of the scanner and time). It makes sense to visualize the acquired data (about 1 GByte in size) in pseudo-3D space, which is feasible on modern computers. Below the results of such a visualization attempt are presented (Fig. 6-7). All the voxels of the 3D space were set to white colour. The magnitude of each data voxel was coded not as the voxels' brightness, but as opacity of the voxel. This makes the white voxels with a low magnitude appear transparent without obscuring the others with large magnitude.

#### **4. Conclusion**

Holographic imaging by means of electrostatic point probe excitation and detection can contribute to the study of the electro-mechanical properties of piezoelectric materials. The method of excitation and detection is simple and versatile. It allows for variation of the frequency of the acoustic waves over a wide range since neither mechanical nor electrical resonances are involved in the coupling scheme. The developed imaging scheme is restricted to piezoelectric materials but not necessarily to single crystals.

The described non-invasive and non-destructive method may find further technical applications. A potential application is the determination of elastic and piezoelectric constants, including elastic constants with rather small values associated with a slight deviation from a higher crystal symmetry class. Furthermore, the imaging scheme may allow for determination of misalignments of the crystal axis with respect to the sample surface. The holographic detection scheme described above is currently employed in a refined scheme for the determination of the elastic constants based on similar methods as already demonstrated for gallium arsenide crystals [12].

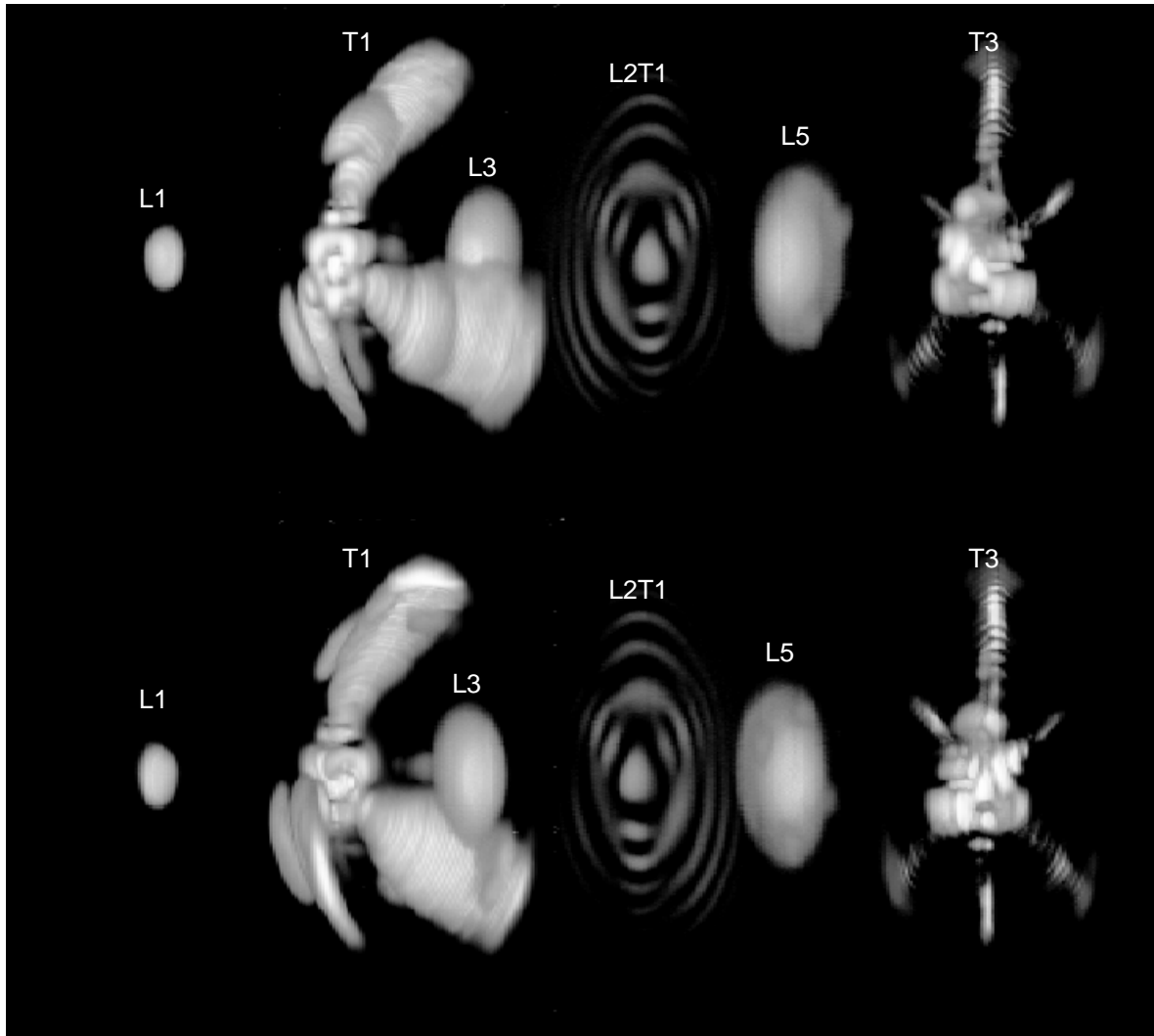


**Fig. 6** Pseudo-3D presentation of the acquired holographic data (magnitude only, coded as opacity of white voxels). The horizontal direction correspond to a total time of  $4,5 \mu\text{s}$ . The labels in the image correspond to those in Fig. 2. The lower image is slightly rotated around the vertical axis to create a rear view of the patterns.

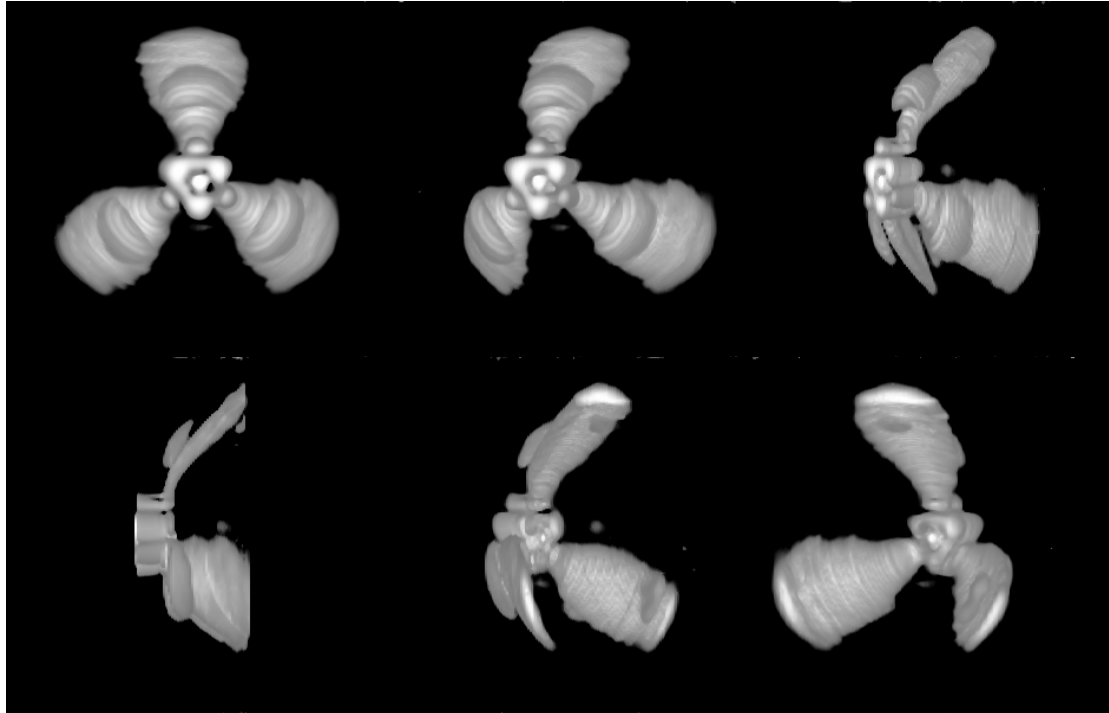


**Fig. 7** First transit signal for transverse polarization (T1 mode in Fig. 2).

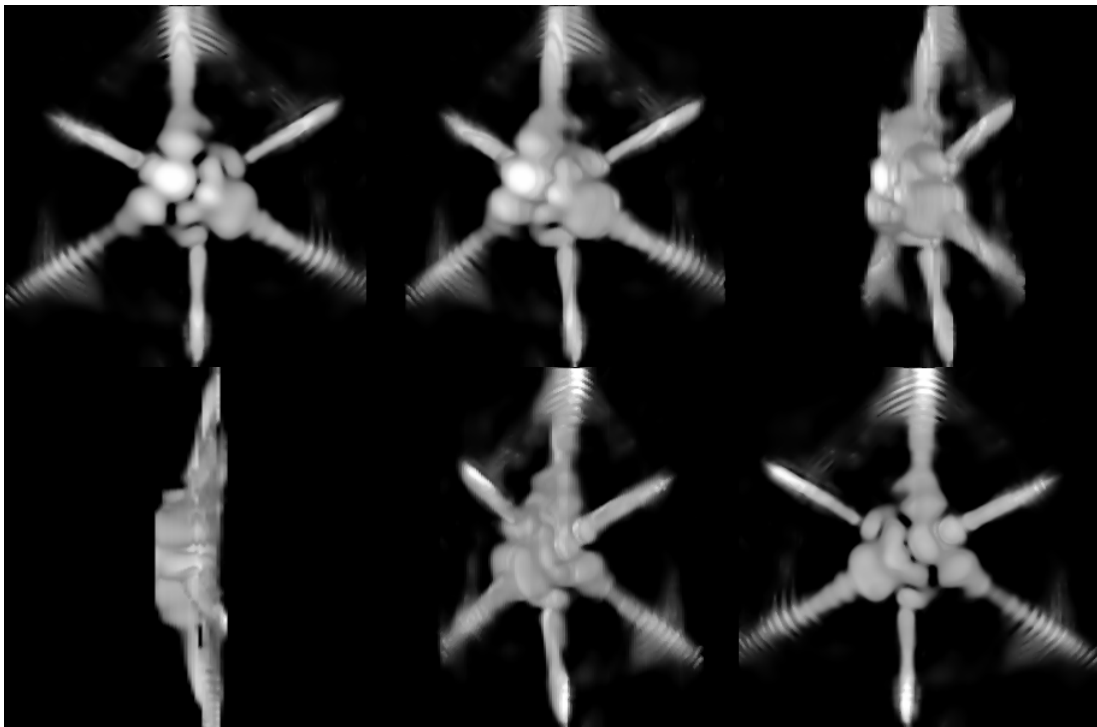


**Fig. 8** One of the later transversally polarized echoes (corresponds to the T7 spike in Fig. 2).

## References

- [1] B. Taylor, H. J. Maris, and C. Elbaum, "Focusing of phonons in crystalline solids due to elastic anisotropy", *Phys. Rev. B* 3, 1462, 1971.
- [2] A. G. Every, "General closed-form expressions for acoustic waves in elastically anisotropic solids", *Phys. Rev. B* 22, 1746, 1980.
- [3] G. L. Koos and J. P. Wolfe, "Phonon focusing in piezoelectric crystals: quartz and lithium niobate", *Phys. Rev. B* 30, 3470, 1984.
- [4] A. G. Every, "Pseudosurface wave structures in phonon imaging" *Phys. Rev. B* 33, 2719, 1986.
- [5] A. G. Every, "Phonon focusing in reflection and transmission", *Phys. Rev. B* 45, 5270, 1992.
- [6] Y. Tanaka, M. Narita, and S. Tamura., "Phonon imaging in superlattices", *J. Phys. C Solid State* 10, 8787, 1998.
- [7] J. P. Wolfe, "Imaging phonons: Acoustic wave propagation in solids", Cambridge University Press, Cambridge, 1998.
- [8] Y. Sugawara, O. B. Wright, O. Matsuda, M. Takigahira, Y. Tanaka, S. Tamura, and E. Gusev, "Watching ripples on crystals", *Phys. Rev. Lett.* 88, 185504, 2002.
- [9] M. R. Hauser, R. L. Weaver, J. P. Wolfe, "Internal diffraction of ultrasound in crystals: phonon focusing at long wavelengths", *Phys. Rev. Lett.*, 68, 2604, 1992.
- [10] B. A. Richardson, G. S. Kino "Probing of elastic surface waves in piezoelectric media", *App. Phys. Lett.* 16, 82, 1970
- [11] W. Grill, K. Hillmann, K. U. Würz and J. Wesner, "Scanning ultrasonic microscopy with phase contrast," in *Advances in Acoustic Microscopy*, A. Briggs and W. Arnold (Editors), vol. 2, New York, 167-218, 1996.
- [12] K. U. Würz, J. Wesner, K. Hillmann, and W. Grill, "Determination of elastic constants using scanning acoustic microscopy", *Z. Phys. B* 97, 487, 1995.